

STUDIES ON THE DISSOCIATION AND UREA-INDUCED UNFOLDING OF FtsZ SUPPORT THE DIMER NUCLEUS POLYMERIZATION MECHANISM

Felipe Montecinos-Franjola, Justin A. Ross, Susana A. Sánchez, Juan E. Brunet, Rosalba Lagos, David M. Jameson and Octavio Monasterio

SUPPORTING MATERIAL

MATERIALS AND METHODS

Protein purification and quantification - FtsZ was overexpressed in *E. coli* BL21 (DE3) strain. Cells were grown at 37°C with agitation in 4 L of LB broth containing 100 $\mu\text{g mL}^{-1}$ ampicillin until an OD_{600} of 0.7 was reached, then 0.4 mM IPTG was added and the cells were grown for additional 4 h. The cells were harvested by centrifugation at $7,000 \times g$ for 45 minutes, the pellet was suspended in buffer A (50 mM Tris-HCl buffer pH 8.0, 50 mM KCl, 1 mM EDTA, and 5% glycerol) and lysed by sonication with five pulses of 45 W (MISONIX 3000, Farmingdale, NY). The lysed cells were centrifuged at $100,000 \times g$ for 90 minutes and the supernatant was saturated with 25% ammonium sulphate. The precipitated protein was centrifuged at $10,000 \times g$ at 4°C, and the pellet was dissolved in buffer A and then dialyzed against 2L of buffer A at 4°C to remove the salt excess. Next, a modification of the purification protocol proposed by Beuria et al. (1), was adapted as follows: three monosodium glutamate polymerization and depolymerization cycles were performed in 50 mM PIPES (pH 6.5), 1 M glutamate, 10 mM CaCl_2 , 10 mM MgCl_2 , and 2 mM GTP for 30 min at 37°C, and the polymers obtained were centrifuged at $10,000 \times g$ for 30 min at 25°C. The protein was solubilized in buffer A and dialyzed to remove the nucleotide excess. The protein concentration and the nucleotide content were determined, respectively, by the Bradford method calibrated for FtsZ and by absorption at 254 and 280 nm using the following extinction coefficients for FtsZ: $\epsilon_{254\text{nm}} = 2,750 \text{ M}^{-1}\text{cm}^{-1}$; $\epsilon_{280\text{nm}} = 3,840 \text{ M}^{-1}\text{cm}^{-1}$ and for the nucleotide GDP: $\epsilon_{254\text{nm}} = 13,700 \text{ M}^{-1}\text{cm}^{-1}$; $\epsilon_{280\text{nm}} = 8,100 \text{ M}^{-1}\text{cm}^{-1}$ (2). The total protein concentration after purification was typically 15-20 mg/mL and the nucleotide content was 0.5-1 mol of GDP per mol of FtsZ.

Preparation of FtsZ conjugates - Fluorescein isothiocyanate (FITC, Sigma, St. Louis, MO), 5-(dimethylamino)naphthalene-1-sulfonyl chloride (DNS, Sigma) and Alexafluor-488 succinimidyl ester (Invitrogen, Carlsbad, CA) were dissolved in dimethylformamide. FtsZ was conjugated with the probes using the traditional protocols. For FITC and DNS labelling, 300 μL of FtsZ (150 μM) were dialyzed against 50 mM potassium phosphate buffer pH 8.4, 50 mM KCl, 1mM EDTA and 5% v/v glycerol at 4°C. For Alexafluor-488 labelling, 300 μL of FtsZ were dialyzed against 50 mM potassium phosphate buffer pH 7, 50 mM KCl, 1mM EDTA and 5% v/v glycerol at 4°C. The dialyzed samples were incubated with a 10-fold molar excess of the dyes at room temperature for 1.5-3 h with occasional agitation. In both cases, the free dye was removed by Sephadex G-25 chromatography (SIGMA) followed by extensive dialysis in 50 mM Tris-HCl buffer pH 8.0, 50 mM KCl, 1 mM EDTA and 5% v/v glycerol. The labelling ratio was determined spectrophotometrically using extinction coefficients of 68,000 and 71,000 $\text{M}^{-1}\text{cm}^{-1}$ at 494-nm for fluorescein derivatives and 3,400 $\text{M}^{-1}\text{cm}^{-1}$ at 340-nm for DNS, respectively. For FtsZ an extinction coefficient of 11,940 $\text{M}^{-1}\text{cm}^{-1}$ at 280-nm was used.

Anisotropy data modelling - Anisotropy data was fit to the two-step equilibrium of association of two monomers (M) into dimers (D) and of two dimers into tetramers (T) (3). The equations describing the model are:

$$2M \xrightleftharpoons{K_{aD}} D; 2D \xrightleftharpoons{K_{aT}} T$$

$$K_{dD} = \frac{1}{K_{aD}}; K_{dT} = \frac{1}{K_{aT}}$$

$$r_{obs} = r_M \alpha_M + r_D \alpha_D + r_T \alpha_T$$

$$1 = \alpha_M + \alpha_D + \alpha_T$$

$$\alpha_M = \frac{1}{1 + 2PK_{aD} + 4P^3 K_{aD}^2 K_{aT}}$$

$$\alpha_D = \frac{2PK_{aD}}{1 + 2PK_{aD} + 4P^3 K_{aD}^2 K_{aT}}$$

$$\alpha_T = \frac{4P^3 K_{aD}^2 K_{aT}}{1 + 2PK_{aD} + 4P^3 K_{aD}^2 K_{aT}}$$

Where K_{dD} and K_{dT} are the dissociation equilibrium constants for dimer and tetramer species, respectively. r_i and a_i are the limiting anisotropies and mole fractions of the species and P is the free monomer concentration. A non-linear regression routine was used in SigmaPlot v.11 (SYSTAT) to fit the experimental data. The quality of the fit was judged by the statistical analyses applied to the fit parameters that are incorporated in the software package.

FtsZ dissociation and unfolding

CD data modelling - Unfolding data was fit with the linear extrapolation method (4,5) using the 3-state dimer intermediate model adapted from previous reports (6-9). The equations describing the model are:

$$\begin{aligned}
 & N_2 \xrightleftharpoons{K_1} I_2 \xrightleftharpoons{K_2} 2U \\
 & CD_{obs} = CD_{N_2} f_{N_2} + CD_{I_2} f_{I_2} + CD_U f_U \\
 & 1 = f_{N_2} + f_{I_2} + f_U \\
 & [U] = \frac{-K_1 K_2 + \sqrt{(K_1 K_2)^2 + 8P(K_1 K_2)(1 + K_1)}}{4(1 + K_1)} \\
 & f_{N_2} = \frac{[U]}{[U] + [U]K_1 + K_1 K_2} \\
 & f_{I_2} = \frac{[U]K_1}{[U] + [U]K_1 + K_1 K_2} \\
 & f_U = \frac{K_1 K_2}{[U] + [U]K_1 + K_1 K_2}
 \end{aligned}$$

N_2 , I_2 and U are the native dimer, intermediate dimer and the unfolded species, respectively. CD_i and f_i are the spectroscopic signals and fractions of the species. K_1 and K_2 are unfolding equilibrium constants in the presence of urea for first and second transitions, respectively. P is the total protein concentration. A non-linear regression routine in SigmaPlot v.11 (SYSTAT) yielded the thermodynamic parameters for each transition. The quality of the fit was judged by the statistical analyses applied to the fit parameters that are incorporated in the software package. The stability of the protein was calculated using the relation $C_{50\%} = (\Delta G_{H_2O}^0)/m$ for the transition that is independent on protein concentration (P) and $C_{50\%} = (\Delta G_{H_2O}^0 + RT \ln P)/m$ for the transition that is dependent on protein concentration.

FCS data analysis - Autocorrelation functions were fit assuming a Gaussian-Lorentzian illumination profile as follows:

$$G(\tau) = \frac{\gamma}{N} \left(1 + \frac{\tau}{\tau_D} \right)^{-1} \left(1 + S^2 \frac{\tau}{\tau_D} \right)^{-\frac{1}{2}}$$

Where $\gamma = 3/(4\pi^2)$ is the scaling factor for the two-photon excitation volume, N is the average particle number, $S = \omega/z$ is the ratio of the axial and radial dimensions of the observation volume, respectively. τ_D is the diffusion time that is related to the diffusion coefficient, D , by $\tau_D = \omega^2/4D$. Values of D calculated from autocorrelation functions were corrected for viscosity changes in solvent due to addition of urea using the relation $D = D_0 \times (\eta_0 / \eta)$ where subscript 0 refers to aqueous solution in the absence of urea. The corrected viscosities were calculated for every urea concentration using the empirical equation (10):

$$\frac{\eta}{\eta_0} = 1 + 3.74 \times 10^{-2} m + 1.78 \times 10^{-3} m^2 - 4.4 \times 10^{-5} m^3$$

Where η_0 is the viscosity of the solution in the absence of urea and η is the viscosity of the solution with urea concentration m , in molality units. From corrected diffusion coefficients, the size of the molecule was calculated using the Stokes-Einstein equation to obtain the hydrodynamic radius, r_H , as:

$$D = \frac{kT}{6\pi\eta r_H}$$

where k is the Boltzmann constant, T is the absolute temperature, η is the viscosity of the solvent and r_H is the Stokes radius of the particle (11).

SUPPORTING MATERIAL TABLES

Table S1 Lifetime and fractional intensities of FtsZ fluorescent conjugates

FtsZ μM	FITC conjugates*				
	τ_1	f_1	τ_2	f_2	$\tau_{\text{ave.}}$
31	0.76 [†] (0.03)	0.08 (<0.01)	3.93 (0.02)	0.92 (<0.01)	3.68
6	0.77 (0.04)	0.07 (<0.01)	3.90 (0.02)	0.93 (<0.01)	3.68
1	0.58 (0.03)	0.08 (<0.01)	3.84 (0.02)	0.92 (<0.01)	3.58
FtsZ μM	DNS conjugates				
	τ_1	f_1	τ_2	f_2	$\tau_{\text{ave.}}$
45	4.27 (0.11)	0.21 (<0.01)	18.5 (0.14)	0.78 (<0.01)	15.2
4	6.19 (0.20)	0.19 (<0.01)	20.2 (0.19)	0.80 (<0.01)	17.3
0.5	5.68 (0.30)	0.14 (0.01)	19.4 (0.20)	0.86 (<0.01)	17.6

*The global reduced chi-square of the fits were $\chi^2=0.7$ and $\chi^2=0.4$ for FITC and DNS conjugates, respectively.

[†]Constant standard errors of 0.2° for phase angle and 0.004 for modulation were used for minimization. Values in parenthesis are the parameters standard errors.

SUPPORTING MATERIAL FIGURES

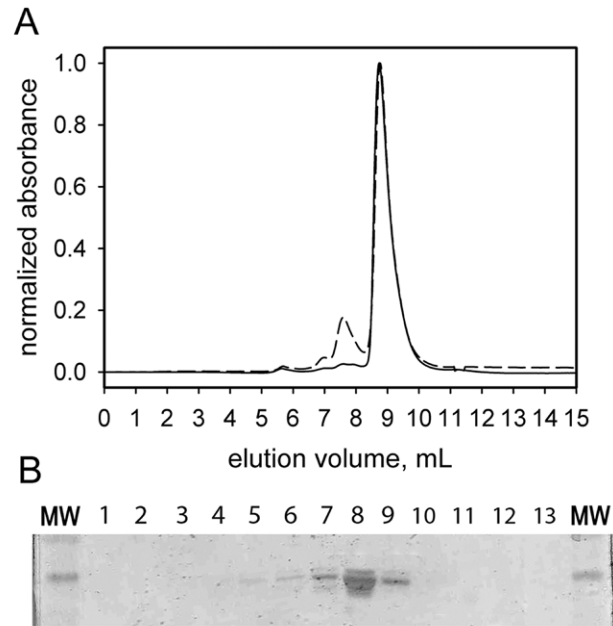


Figure S1. *A* SEC profile of FtsZ wild type (3 μM, solid line) and FtsZ-FITC (13 μM, dashed line) as mentioned in the main text. The observed proportions of the species in the labelled protein: monomer 80%, dimer 14% and tetramer 6%. *B* silver stained 12% SDS-PAGE of fractions (1 mL) collected directly from detector outlet. The numbers on the top show the volume of elution corresponding to the collected fractions. MW, molecular weight standard.

FtsZ dissociation and unfolding

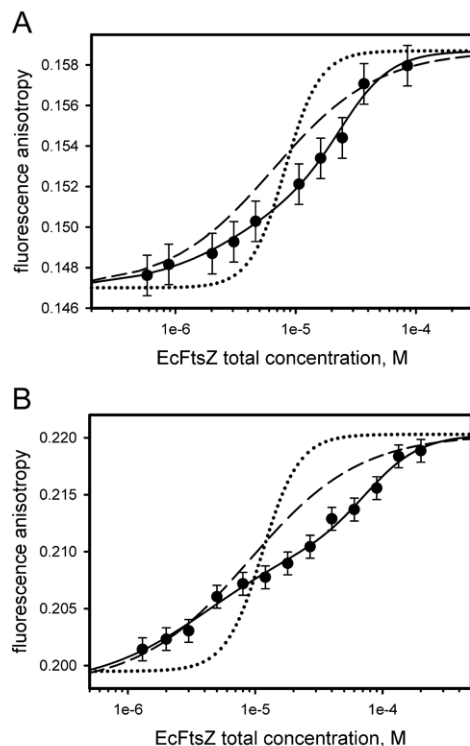


Figure S2. *A* FtsZ-FITC anisotropy data from dilution experiments (*solid circles*). The *solid line* represents the simulation of the 3-states dissociation equilibrium from tetramers to monomers through a dimer intermediate ($2M \leftrightarrow D$; $2D \leftrightarrow T$) with dissociation constants $K_{dD} = 9 \times 10^{-6}$ M and $K_{dT} = 152 \times 10^{-6}$ M (see main text). The *dashed line* shows the simulation of the 2-states dissociation of dimers into monomers ($2M \leftrightarrow D$) with a *dissociation* constant $K_{dD} = 13 \times 10^{-6}$ M. The *dotted line* shows the simulation of the 2-states dissociation of tetramers into monomers ($4M \leftrightarrow T$) using a dissociation constant $K_{dT} = 2 \times 10^{-15}$ M³. *B* FtsZ-DNS anisotropy data from dilution experiments (*solid circles*). The *solid line* represents the simulation of the 3-states dissociation equilibrium from tetramers to monomers through a dimer intermediate ($2M \leftrightarrow D + 2D \leftrightarrow T$) with dissociation constants $K_{dD} = 8 \times 10^{-6}$ M and $K_{dT} = 1500 \times 10^{-6}$ M. The *dashed line* corresponds to the simulation of the 2-states dissociation of dimers into monomers ($2M \leftrightarrow D$) with dissociation constant $K_{dD} = 18 \times 10^{-6}$ M. The *dotted line* shows the simulation of the 2-states dissociation of tetramers into monomers ($4M \leftrightarrow T$) using a dissociation constant $K_{dT} = 5.8 \times 10^{-15}$ M³. The limiting anisotropies for the monomer, dimer and tetramer species in each case were chosen to facilitate comparison.

FtsZ dissociation and unfolding

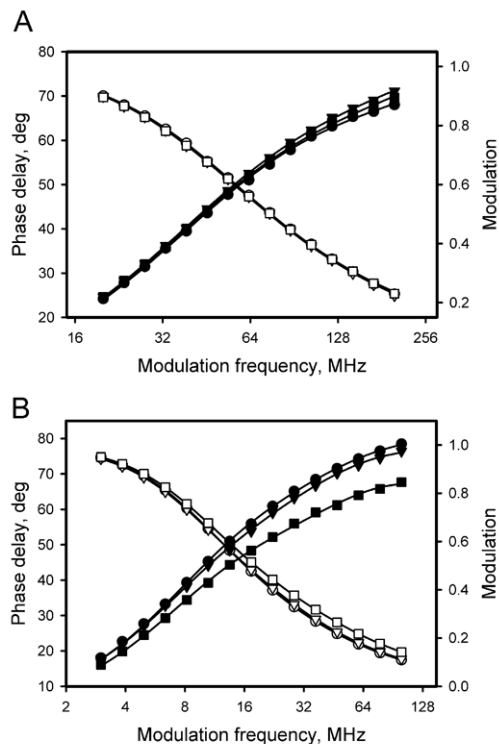


Figure S3. Frequency domain lifetime data showing the phase delay angle (*closed symbols*) and the modulation ratio (*open symbols*) of the fluorescence emission in 50 mM potassium phosphate buffer pH 6.5 at 22 °C. *A.* Lifetime measurements of FtsZ-FITC conjugates at 31 μM (*squares*), 6 μM (*triangles*) and 1 μM (*circles*) of total protein concentration. *B.* Lifetime measurements of FtsZ-DNS conjugates at 45 μM (*squares*), 4 μM (*triangles*) and 0.5 μM (*circles*) of total protein concentration. The *solid lines* represent the fits to the experimental data with lifetimes and fractional intensities summarized in table S1.

FtsZ dissociation and unfolding

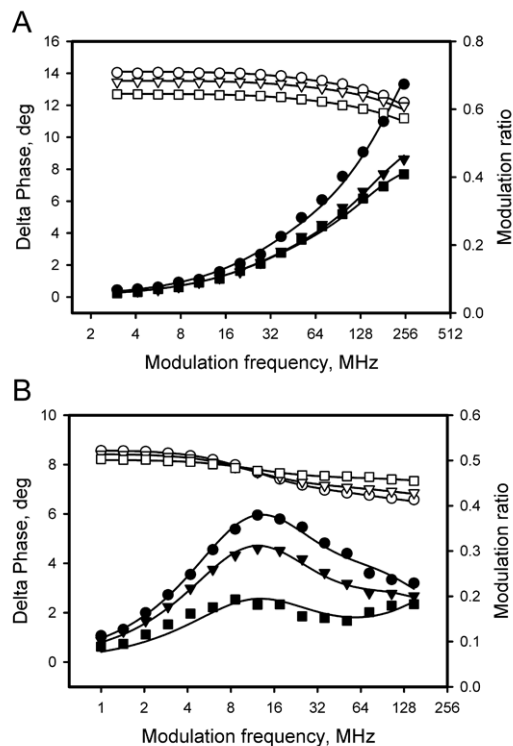


Figure S4. Dynamic polarization data of the fluorescence as a function of total protein concentration in 50 mM potassium phosphate buffer pH 6.5 at 22°C. The differential phase angle (*closed symbols*) and the amplitude ratio (*open symbols*) are shown as a function of modulation frequency. *A.* Measurements of FtsZ-FITC conjugates at 31 μM (*squares*), 6 μM (*triangles*) and 1 μM (*circles*). *B.* Measurements of FtsZ-DNS conjugates at 45 μM (*squares*), 4 μM (*triangles*) and 0.5 μM (*circles*). The *solid lines* represent the fits to the experimental data with average lifetimes, rotational correlation times and fractional anisotropies summarized in table 2 in the main text.

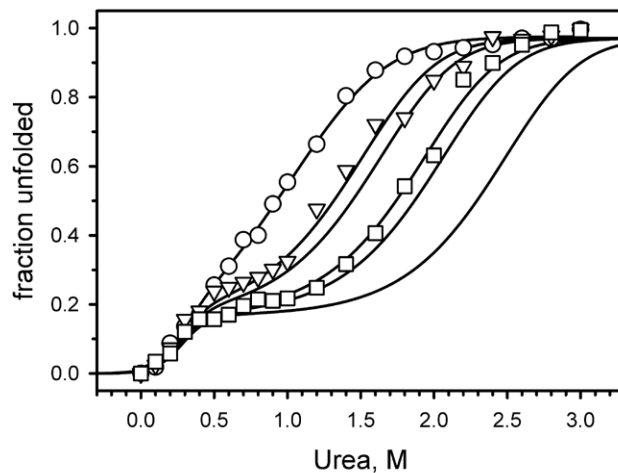


Figure S5. Theoretical values (*solid lines*) obtained from the 3-states dimer unfolding model at (from left to right) 1, 5.6, 15, 46.3, 150 and 1500 μM of protein concentration, respectively. The *open symbols* at 1 μM (*circles*), 5.6 μM (*triangles*) and 46.3 μM (*squares*) represent the experimental data from CD experiments as shown in figure 4 *A*. The theoretical values were calculated using the data from the 3-states dimer global fit informed in table 4.

FtsZ dissociation and unfolding

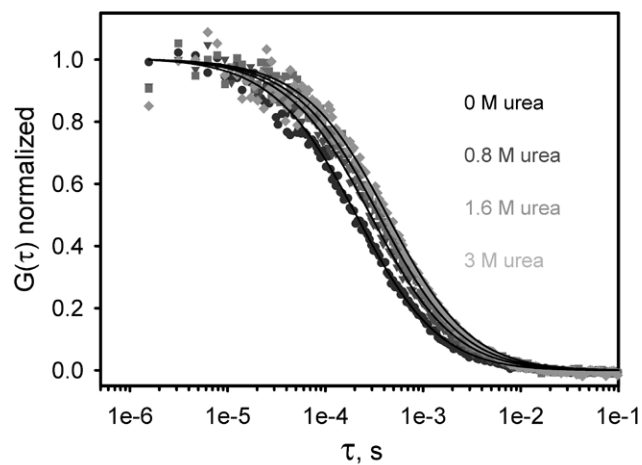


Figure S6. Normalized fluorescence autocorrelation functions of FtsZ-Alexa488 (100 nM) at four urea concentrations (from left to right): 0 M (*black*), 0.8 M (*dark grey*), 1.6 M (*medium grey*) and 3 M (*light grey*) in 50 mM potassium phosphate buffer pH 6.5 at room temperature. The *solid lines* represent the fit autocorrelation functions using one diffusion component.

SUPPORTING MATERIAL REFERENCES

1. Beuria, T. K., S. S. Krishnakumar, S. Sahar, N. Singh, K. Gupta, M. Meshram, and D. Panda. 2003. Glutamate-induced assembly of bacterial cell division protein FtsZ. *J Biol Chem* 278:3735-3741.
2. Andreu, J. M., M. A. Oliva, and O. Monasterio. 2002. Reversible Unfolding of FtsZ Cell Division Proteins from Archaea and Bacteria. *The Journal of Biological Chemistry* 277:43262-43270.
3. Bujalowski, W. and T. M. Lohman. 1991. Monomer-tetramer equilibrium of the *Escherichia coli* ssb-1 mutant single strand binding protein. *J Biol Chem* 266:1616-1626.
4. Pace, C. N. 1986. Determination and analysis of urea and guanidine hydrochloride denaturation curves. *Methods Enzymol* 131:266-280.
5. Santoro, M. M. and D. W. Bolen. 1988. Unfolding free energy changes determined by the linear extrapolation method. 1. Unfolding of phenylmethanesulfonyl alpha-chymotrypsin using different denaturants. *Biochemistry* 27:8063-8068.
6. Bowie, J. U. and R. T. Sauer. 1989. Equilibrium dissociation and unfolding of the Arc repressor dimer. *Biochemistry* 28:7139-7143.
7. Hobart, S. A., D. W. Meinhold, R. Osuna, and W. Colon. 2002. From two-state to three-state: the effect of the P61A mutation on the dynamics and stability of the factor for inversion stimulation results in an altered equilibrium denaturation mechanism. *Biochemistry* 41:13744-13754.
8. Fu, L. and J. J. Liang. 2002. Unfolding of human lens recombinant betaB2- and gammaC-crystallins. *J Struct Biol* 139:191-198.
9. Neet, K. E. and D. E. Timm. 1994. Conformational stability of dimeric proteins: Quantitative studies by equilibrium denaturation. *Protein Science* 3. :2167-2174
10. Kawahara, K. and C. Tanford. 1966. Viscosity and density of aqueous solutions of urea and guanidine hydrochloride. *J Biol Chem* 241:3228-3232.
11. Jameson, D. M., J. A. Ross, and J. P. Albanesi. 2009. Fluorescence fluctuation spectroscopy: ushering in a new age of enlightenment for cellular dynamics. *Biophys Rev* 1:105-118.